Electronic Supplementary Information (ESI) for Analytical Methods

Electronic Supplementary Information

Geometrically controlled preparation of various cell aggregates by droplet-based microfluidics

Yaolei Wang,[a] Lei Zhao,[b] Chang Tian,[b] Chao Ma,[b] and Jinyi Wang*[a,b]

[a] *College of Science, Northwest A&F University, Yangling, Shaanxi 712100, P. R. China*

[b] *College of Veterinary Medicine, Northwest A&F University, Yangling, Shaanxi 712100, P. R. China*

Abstract. This Supplementary data include all of the additional information as noted in the manuscript.

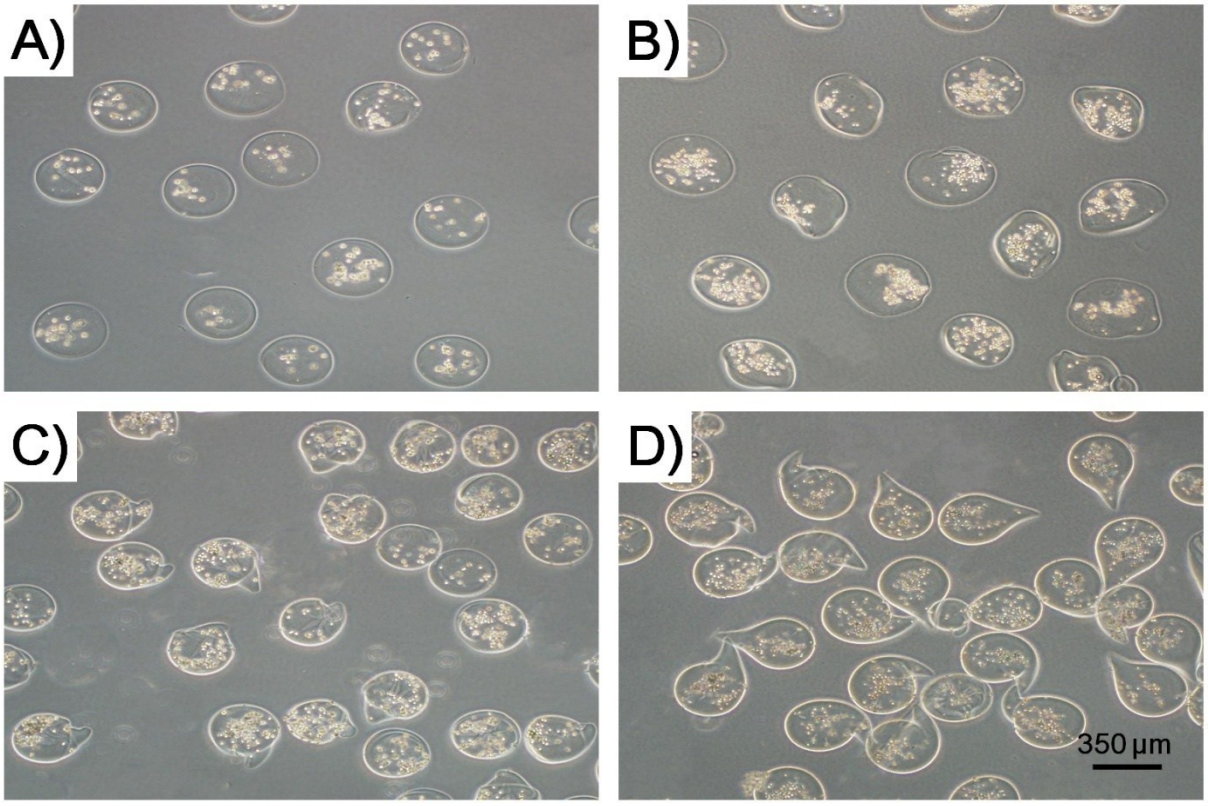

Fig. S1. Phase contrast images of Ca-alginate microparticles containing HeLa cells, formed by crosslinking 0.5% (A), 1% (B), 2% (C), and 3% (D) alginate with 5% $CaCl_2$, respectively**.**

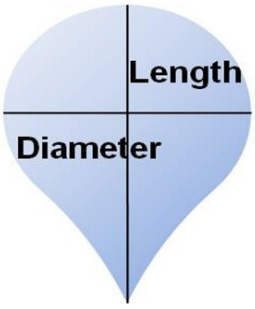

Fig. S2. To facilitate the quantitative analysis of the tail-shaped microparticles, the diameter and length of the microparticles were calculated as described in this figure.

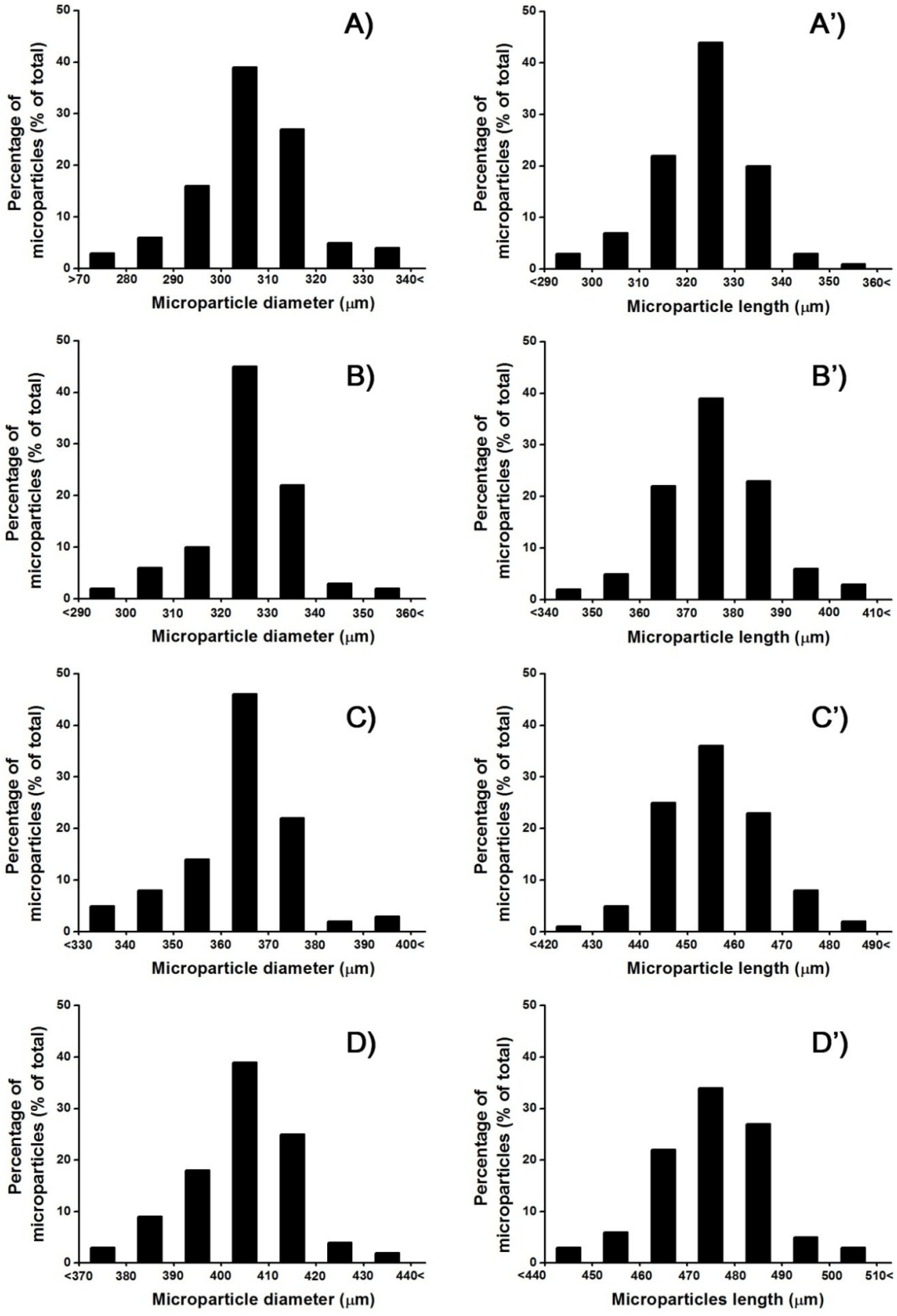

Fig. S3. Statistical graphs of the diameter and length distributions of Ca-alginate microparticles, formed by crosslinking 0.5% (A and A'), 1% (B and B'), 2% (C and C'), and 3% (D and D') alginate with 5% $CaCl_2$, respectively.

Table S1. Statistical analysis of the diameter and length Ca-alginate microparticles formed by crosslinking 0.5%, 1%, 2%, and 3% alginate with 5% $CaCl_2$, respectively (n=100).

Alginate (%)	Diameter (μm)	Length (μm)
0.5	314.95±15.38	320.80±19.69
1	330.69 ±17.51	398.52±25.21
2	368.08 ±16.83	458.72±24.16
3	410.46±19.12	482.59±19.61

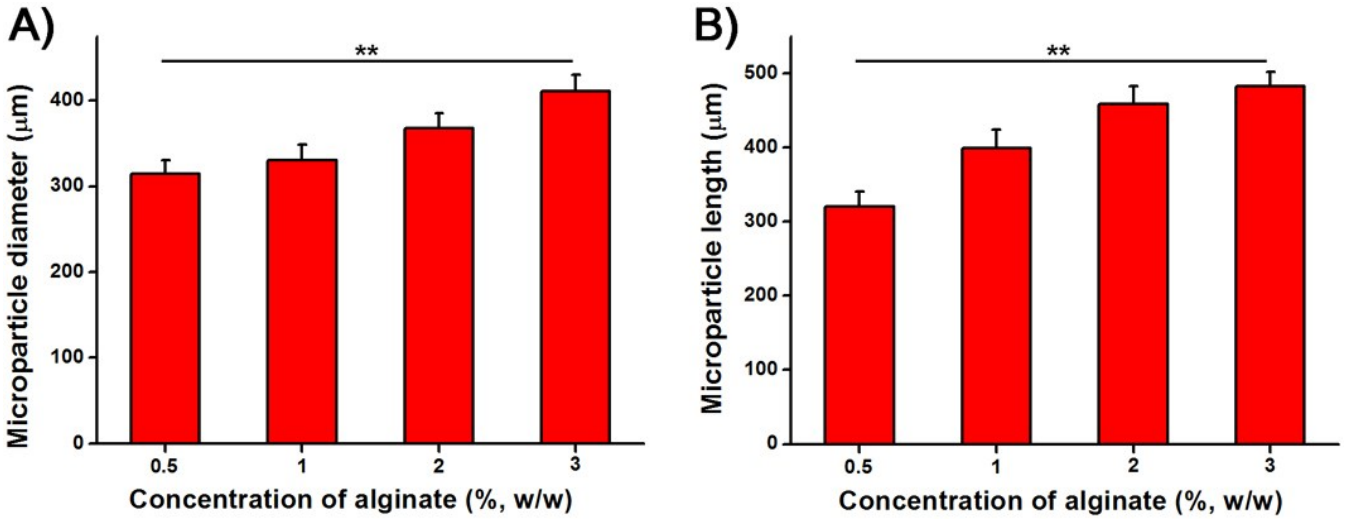

Fig. S4. Statistical analysis of the diameter (A) and length (B) of Ca-alginate microparticles formed by crosslinking 0.5%, 1%, 2%, and 3% alginate with 5% $CaCl_2$, respectively. Data are presented as the mean ± SD, n = 100, with significance assessed by ANOVA. ** $p < 0.001$.

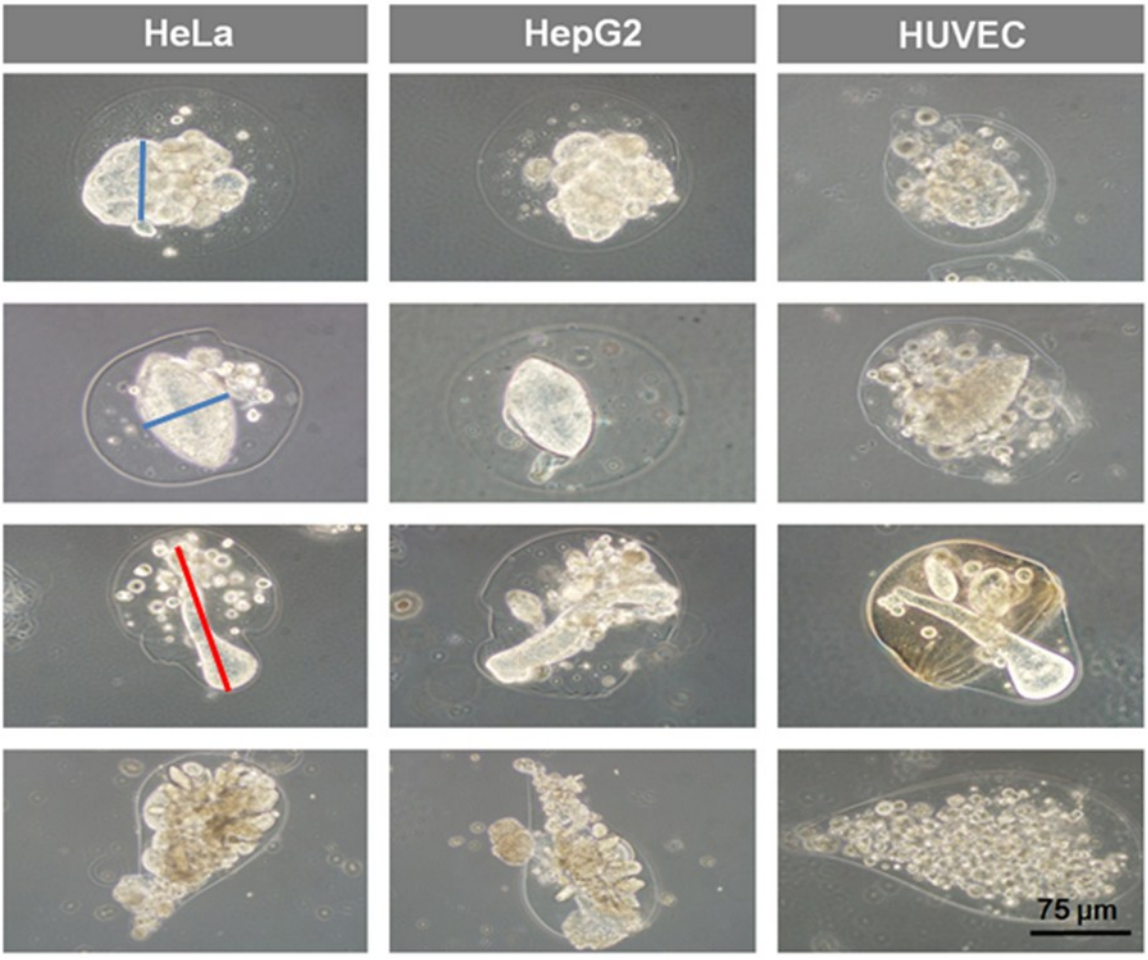

Fig. S5. Typical phase contrast images of HeLa, HepG2 and HUVEC cell aggregates after culture 96 h in different Ca-alginate microparticles formed (from top to bottom) by crosslinking 0.5% (the first row), 1% (the second row), 2% (the third row), and 3% (the fourth row) alginate with 5% $CaCl_2$, respectively. The blue lines defined the diameter of the spherical and spindle-like cell aggregates and the red line defined the length of the branch-like cell aggregates.

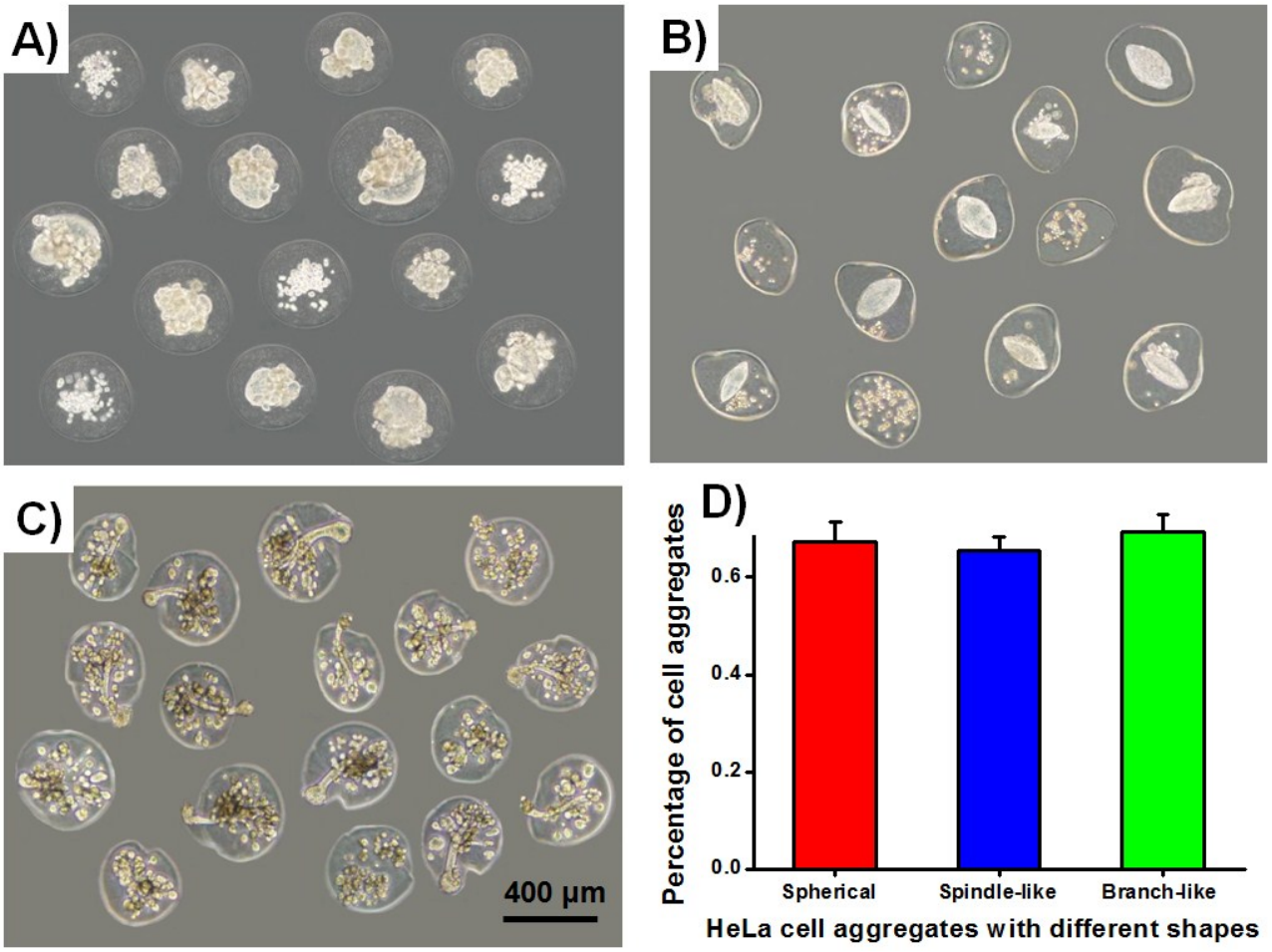

Fig. S6. Typical images of HeLa cell aggregates with spherical (A), spindle-like (B) and branch-like (C) shapes formed in their corresponding microbeads. D) Statistical analysis of different shape cell aggregates formed in their corresponding microbeads (n=50).

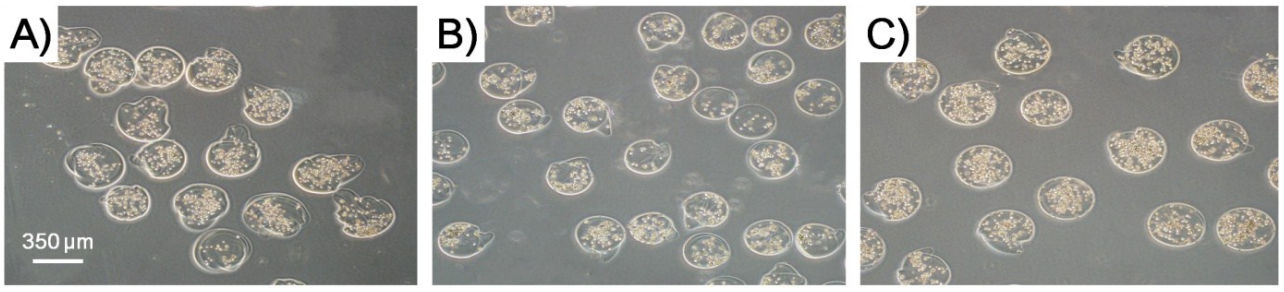

Fig. S7. Phase contrast images of Ca-alginate microparticles containing HeLa cells, formed by crosslinking 2.5% (A), 5% (B), and 10% (C) $CaCl_2$ with 2% alginate, respectively.

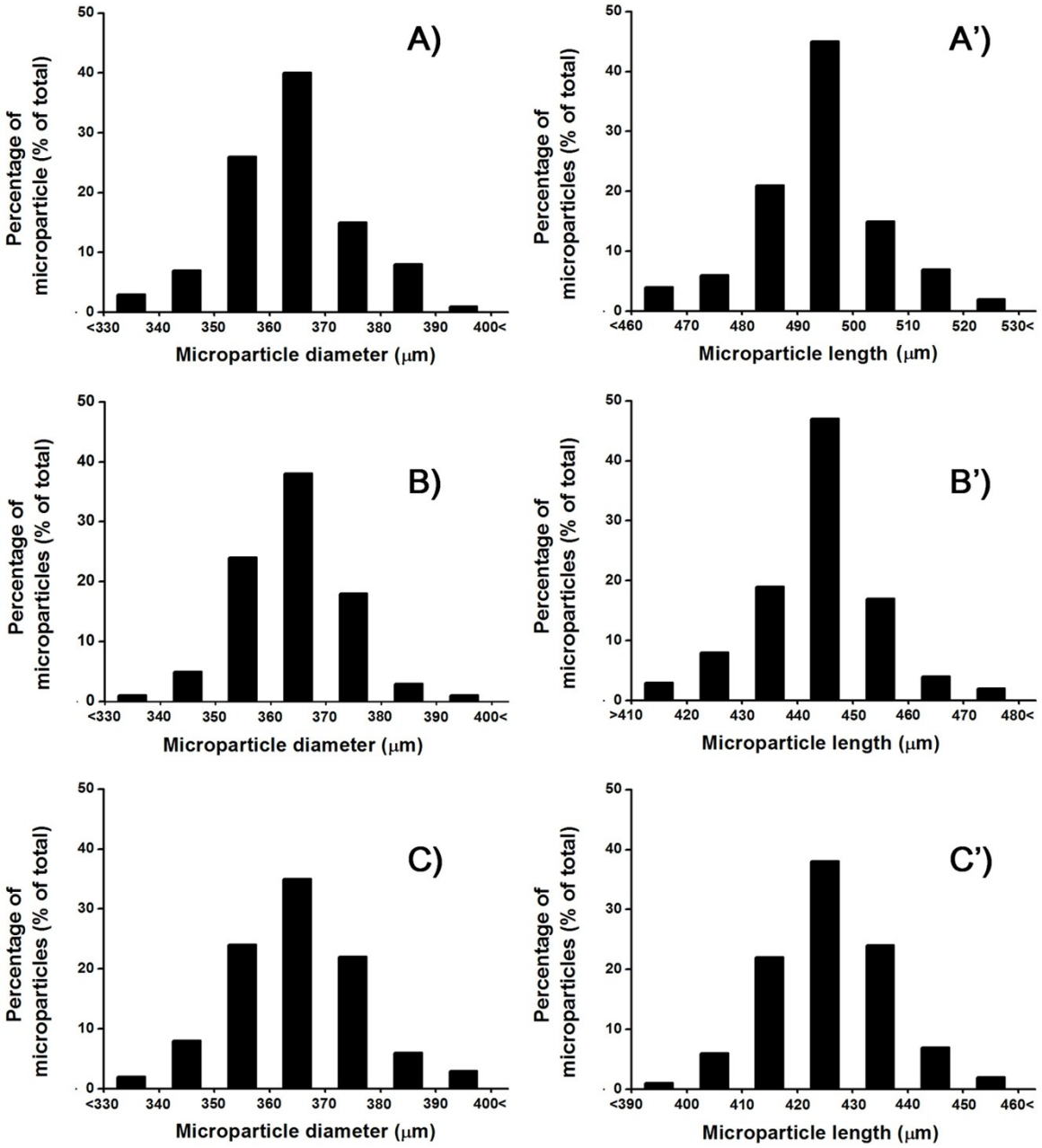

Fig. S8. Statistical graphs of the diameter and length distributions of Ca-alginate microparticles, formed by crosslinking 2.5% (A and A'), 5% (B and B'), and 10% (C and C') $CaCl_2$ with 2% alginate, respectively.

Table S2. Statistical analysis of the diameter and length of Ca-alginate microparticles formed by crosslinking 2.5%, 5%, and 10% $CaCl_2$ with 2% alginate, respectively (n=100).

$CaCl_2$ (%)	Diameter (μm)	Length (μm)
2.5	366.08±13.38	495.72±18.69
5	368.35±14.51	446.72±19.21
10	367.38±15.83	425.26±17.16

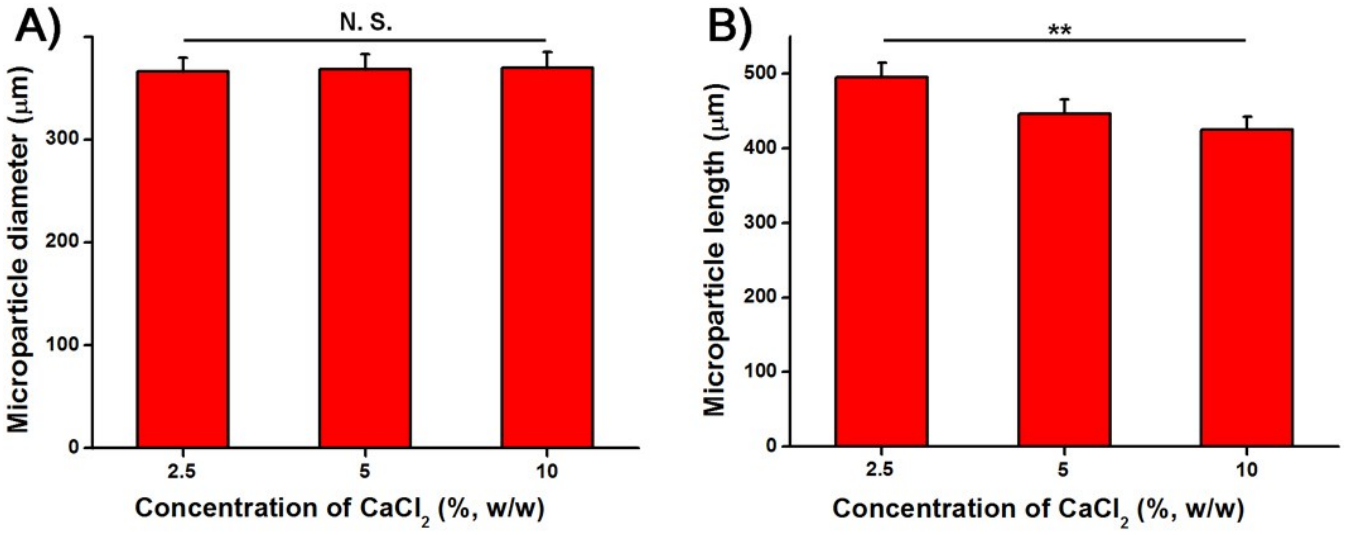

Fig. S9. Statistical analysis of the diameter (A) and length (B) of Ca-alginate microparticles formed by crosslinking 2.5%, 5%, and 10% $CaCl_2$ with 2% alginate, respectively. Data are presented as the mean ± SD, n = 100, with significance assessed by ANOVA. ** $p < 0.001$; N.S., not significant.

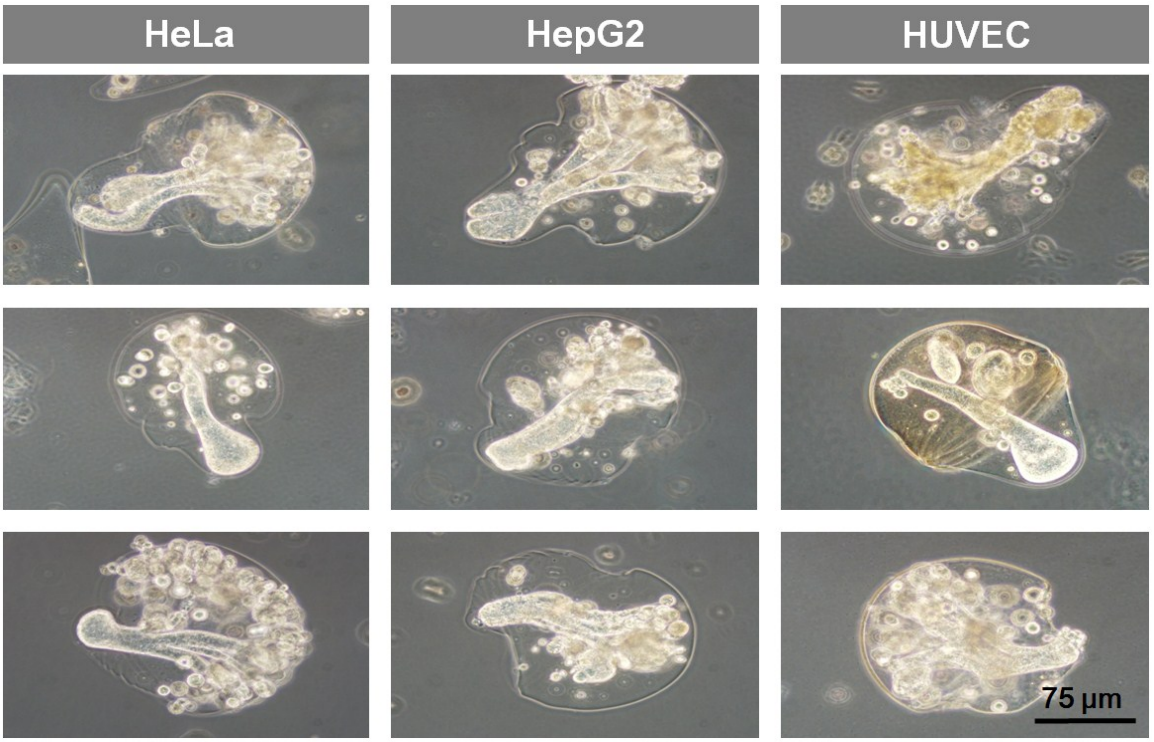

Fig. S10. Typical phase contrast images of HeLa, HepG2 and HUVEC cell aggregates after culture 96 h in different Ca-alginate microparticles formed (from top to bottom) by crosslinking 2.5% (the first row), 5% (the second row), and 10% (the third row) $CaCl_2$ with 2% alginate, respectively.

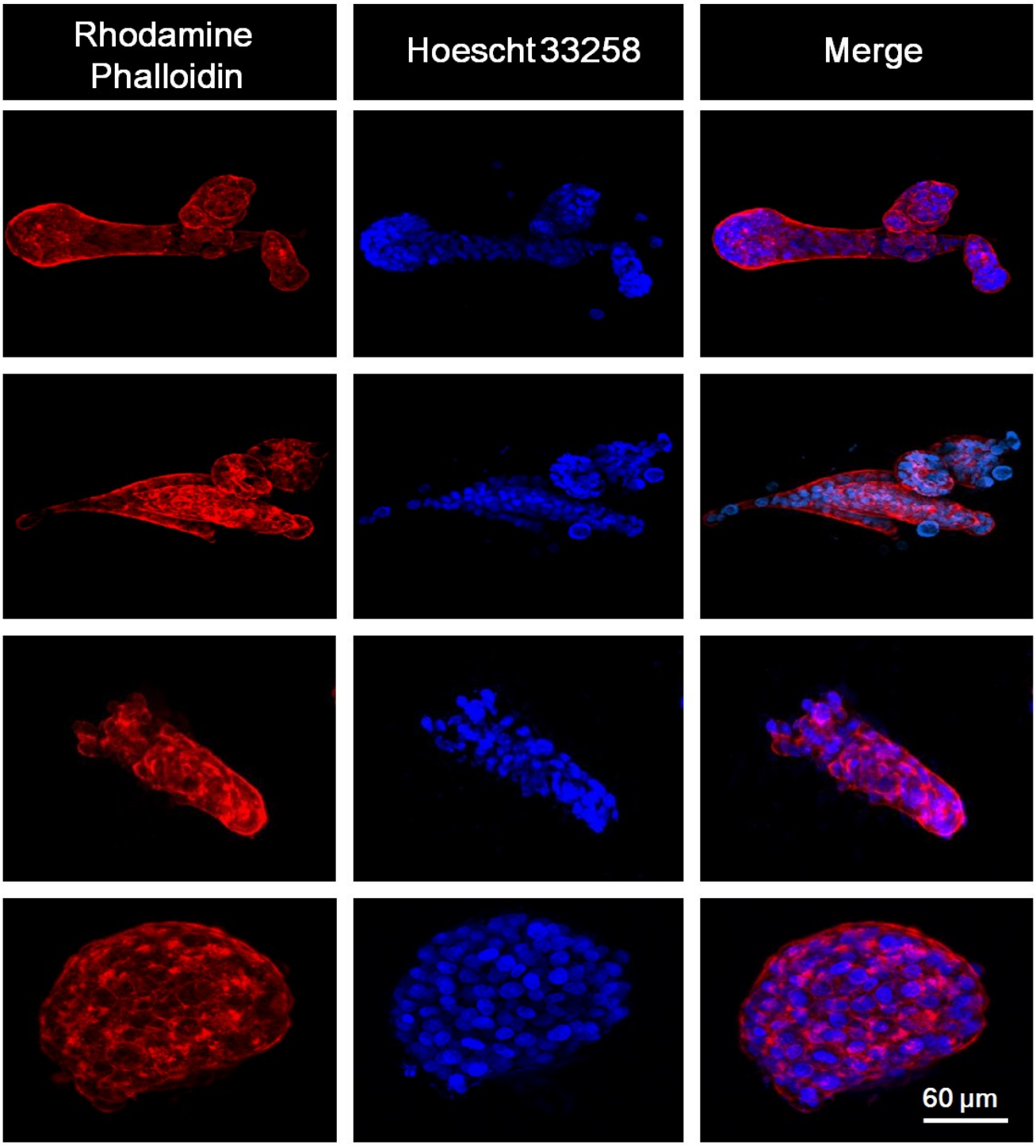

Fig. S11. Fluorescence images of the different shapes of HeLa cell aggregates formed in their corresponding microparticles. From top to bottom: the concentrations of alginate and $CaCl_2$ used for the formation of the corresponding microparticles were 2% and 5% (the first row), 2% and 2.5% (the second row), 1% and 5% (the third row), and 0.5% and 5% (the fourth row), respectively. Cell aggregates were stained with rhodamine phalloidin (red) and Hoechst 33258 (blue).

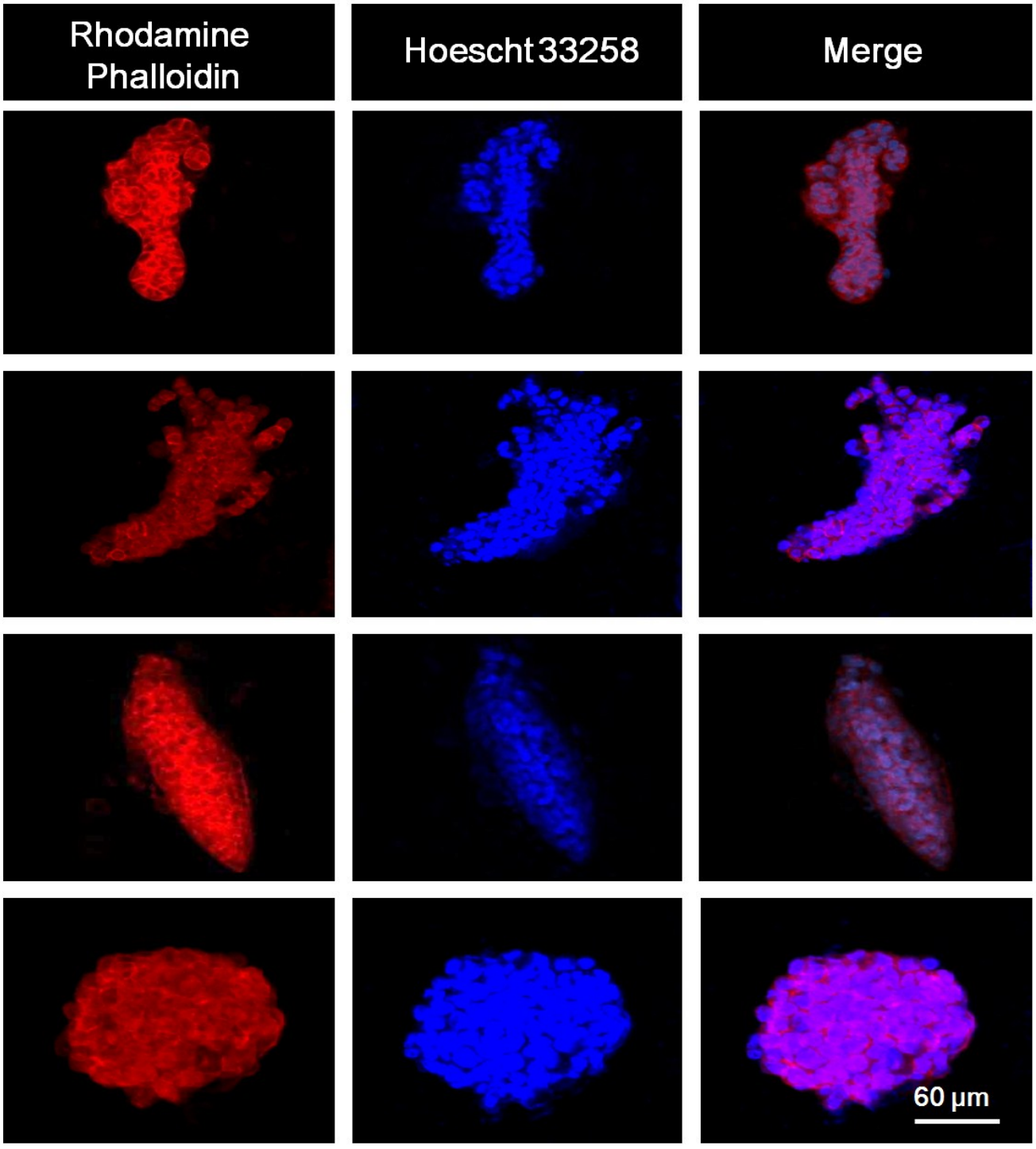

Fig. S12. Fluorescence images of the different shapes of HepG2 cell aggregates formed in their corresponding microparticles. From top to bottom: the concentrations of alginate and $CaCl_2$ used for the formation of the corresponding microparticles were 2% and 5% (the first row), 2% and 2.5% (the second row), 1% and 5% (the third row), and 0.5% and 5% (the fourth row), respectively. Cell aggregates were stained with rhodamine phalloidin (red) and Hoechst 33258 (blue).

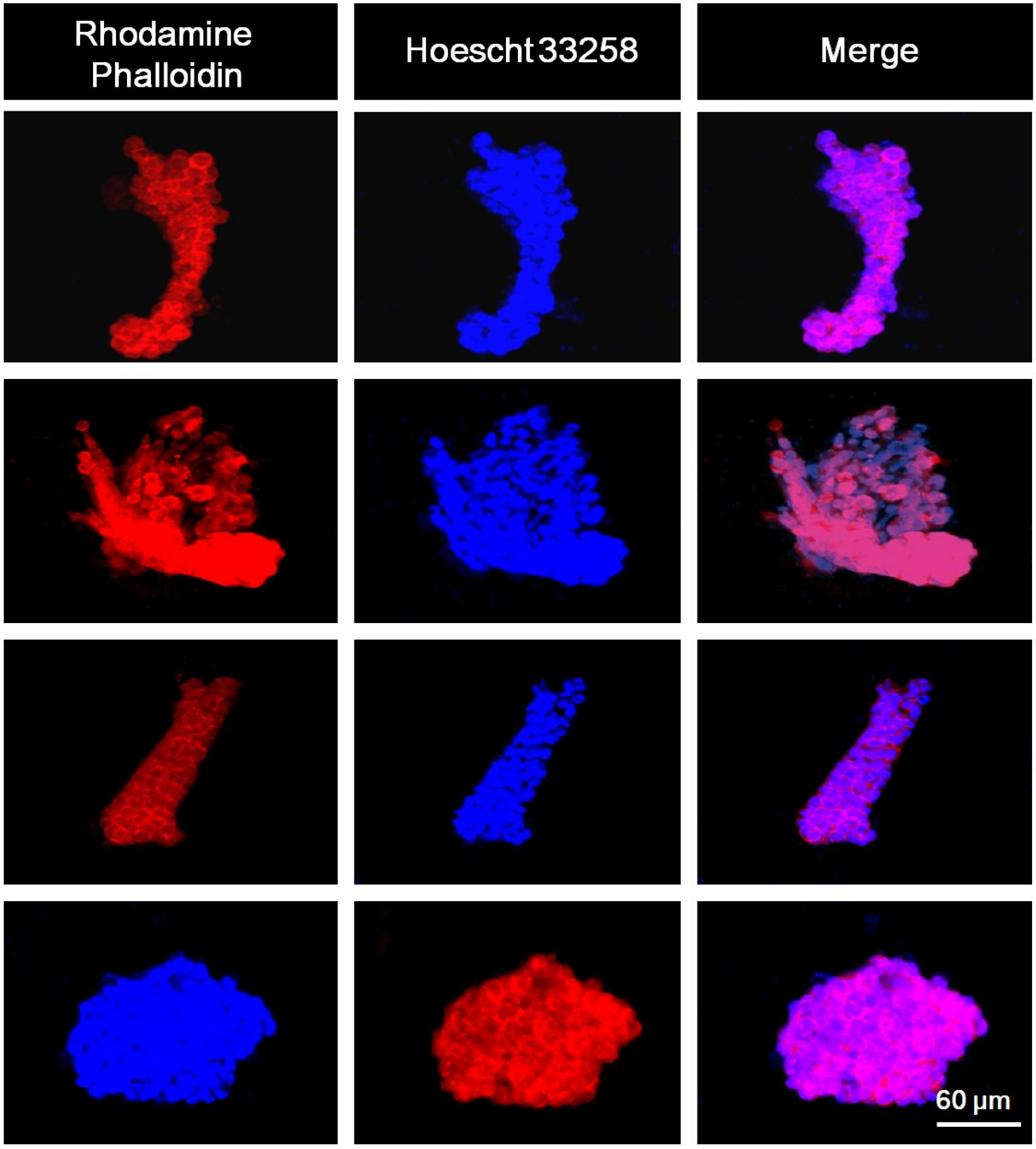

Fig. S13. Fluorescence images of the different shapes of HUVEC aggregates formed in their corresponding microparticles. From top to bottom: the concentrations of alginate and $CaCl_2$ used for the formation of the corresponding microparticles were 2% and 5% (the first row), 2% and 2.5% (the second row), 1% and 5% (the third row), and 0.5% and 5% (the fourth row), respectively. Cell aggregates were stained with rhodamine phalloidin (red) and Hoechst 33258 (blue).

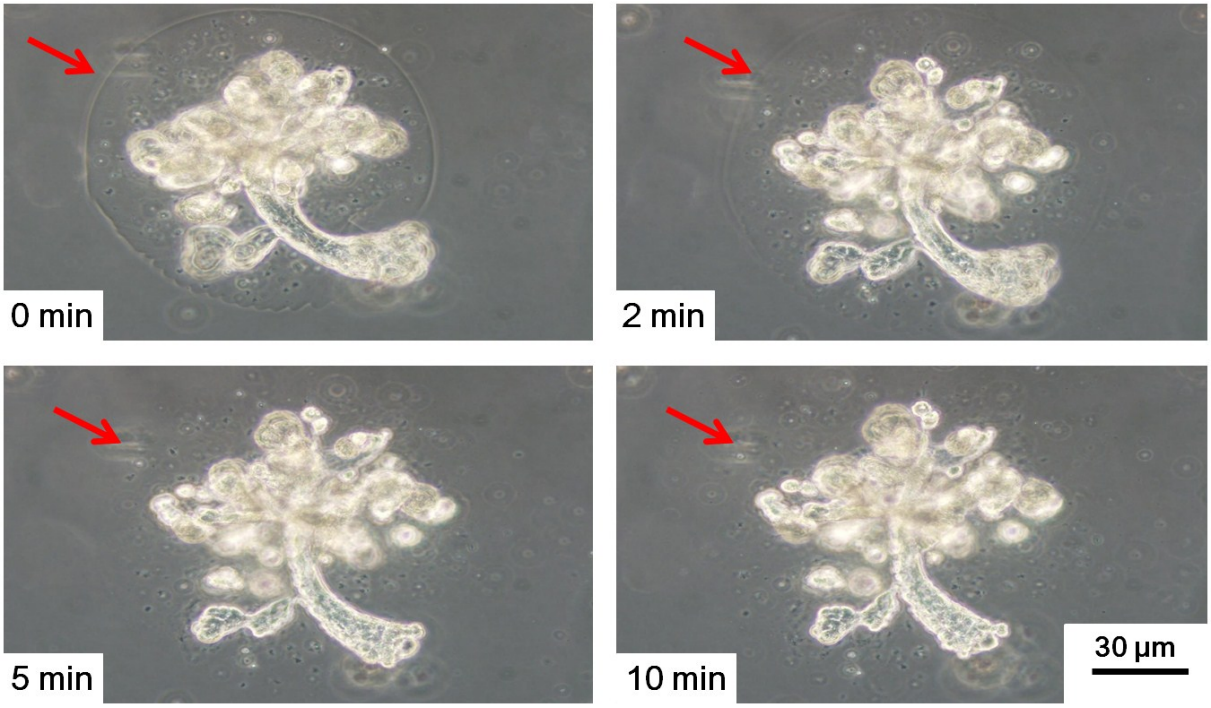

Fig. S14. Time-sequence images of the retrieval of HeLa cell aggregates from Ca-alginate microparticles. As time passed, Ca-alginate microparticles were dissolved gradually (red arrow). After 10 min, the Ca-alginate microparticles were dissolved completely.

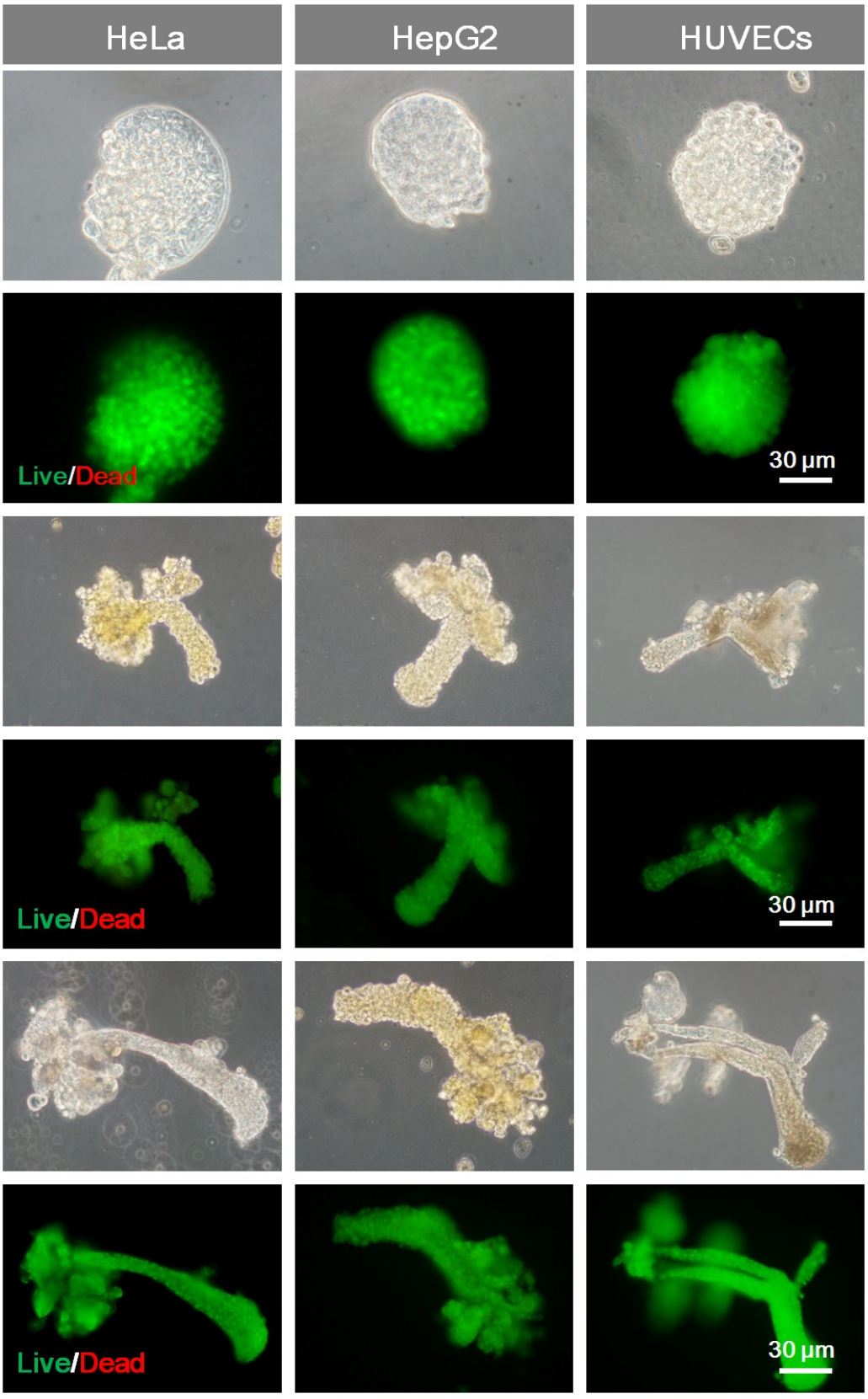

Fig. S15. Typical phase contrast and fluorescence image of HeLa, HepG2 and HUVEC cell aggregates with different shapes after releasing from the Ca-alginate microparticles.

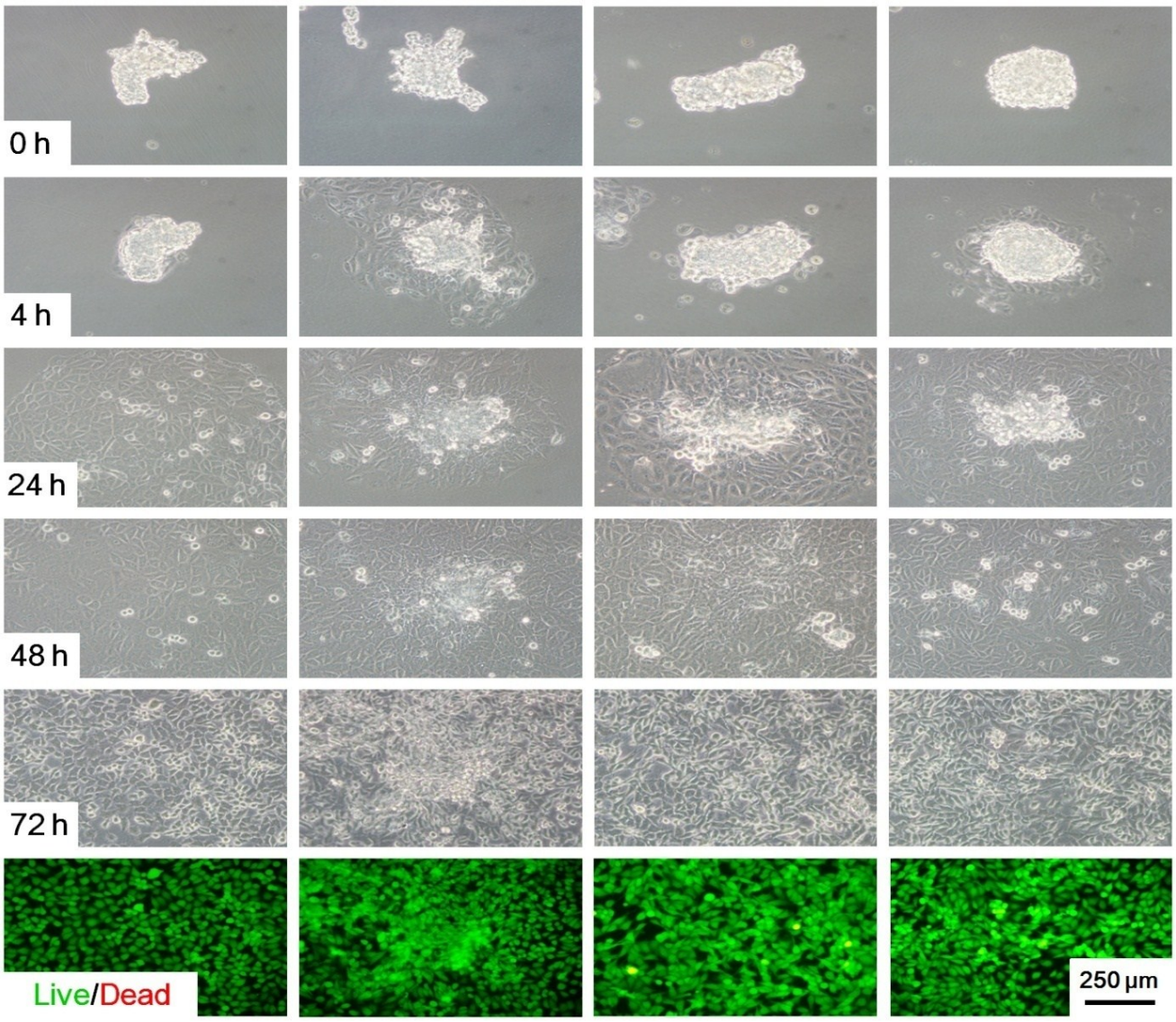

Fig. S16. Time-sequence images of the proliferation and viability of the retrieved HeLa cells cultured in standard culture plates.

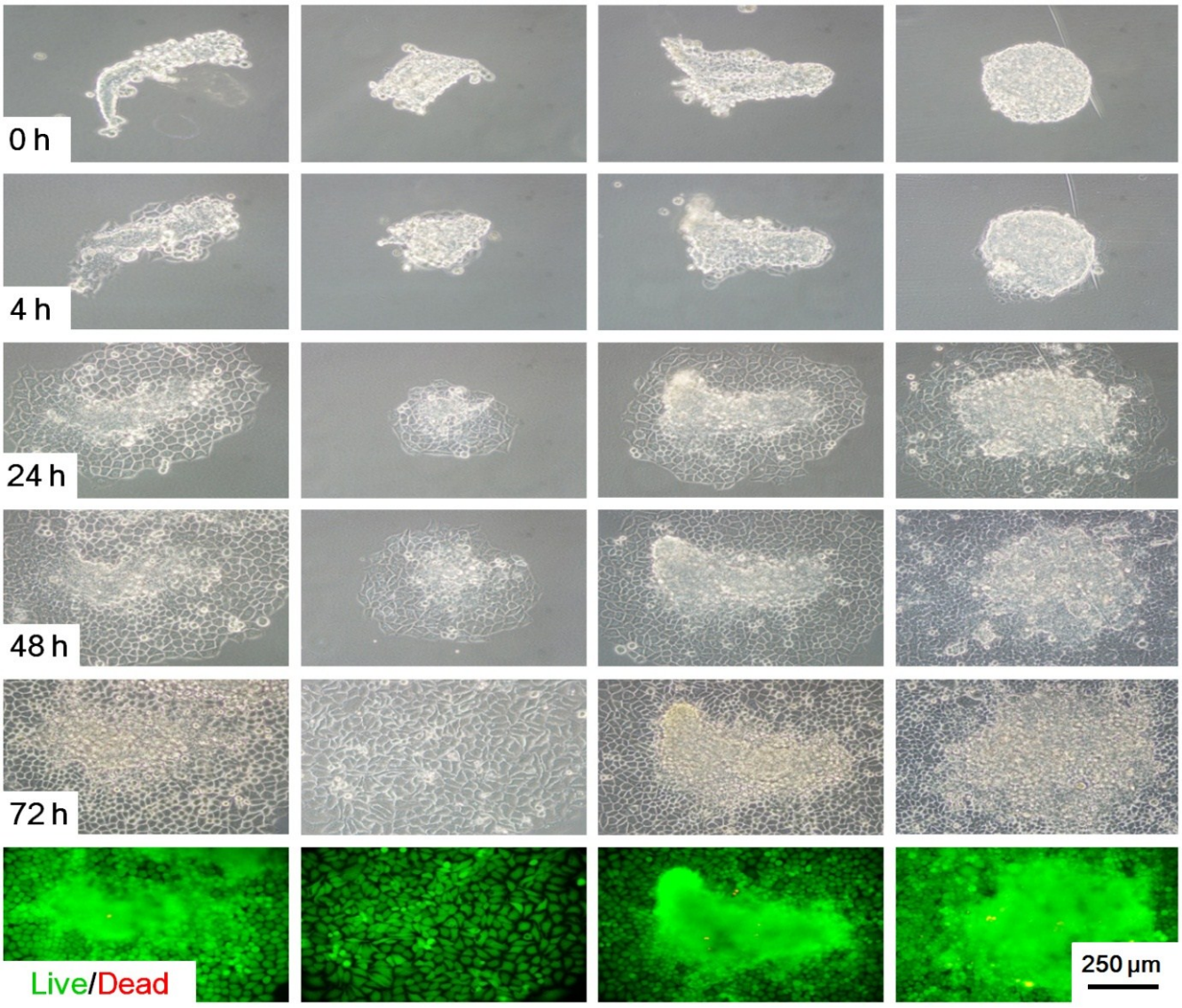

Fig. S17. Time-sequence images of the proliferation and viability of the retrieved HepG2 cells cultured in standard culture plates.

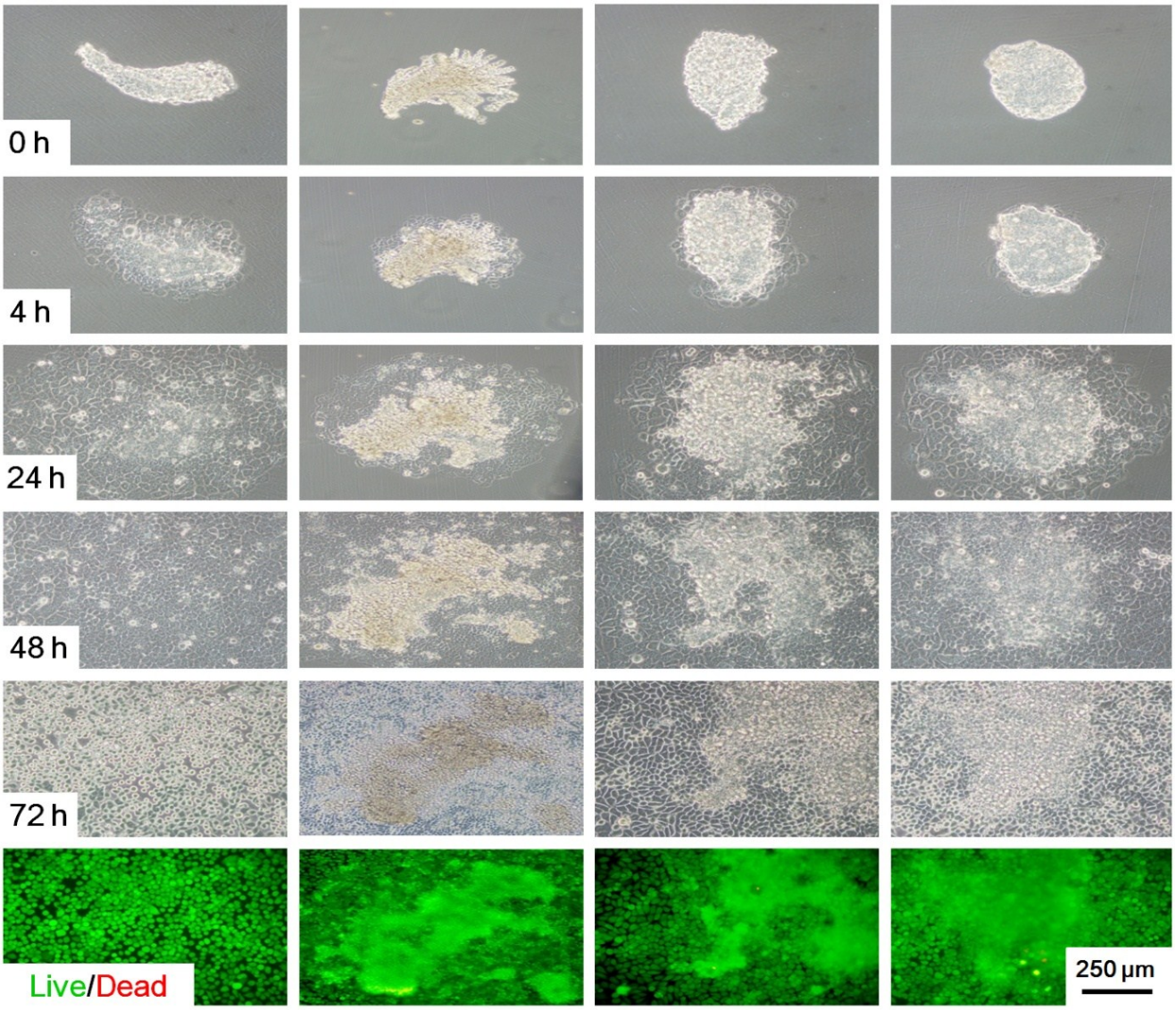

Fig. S18. Time-sequence images of the proliferation and viability of the retrieved HUVECs cultured in standard culture plates.